Electrical Conductivity and Magnetic Properties Studies of Chromium Substitutedlithium Nano Ferrites

D. Ravinder Nayak[#], Poornima. B. Shetty[*], D. Ravinder[#]

[#]*Department of Physics, Osmania University, Hyderabad, Telangana, India*
[*] *C.V.R College of Engineering, Ibrahimpatnam, R.R dist., Telangana, India*
Corresponding Author: *Poornima. B. Shetty*

***Abstract*: The structure and electrical properties of Li-Cr spinel ferrite prepared by the citrate gel auto combustion technique, X-ray diffraction carried out to confirm the formation of the single phase cubic spinel structure. Electrical conductivity of lithium-chromium (Li-Cr) Nano ferrites of various composition have been investigated as a function of composition and temperature. A room temperature magnetization result shows a ferromagnetic behaviour decreases with increase in chromium content. The detailed results of structural and magnetic have been discussed so as to bring out the role of Cr substitution in lithium ferrite.**

Key words: Spinel ferrites, Citrate gel method, magnetic stirrer, XRD and Thermal activation energy

I. INTRODUCTION

Ferrites have potential applications in electrical components, memory devices and microwave devices over a wide range of frequencies because of their high resistivity and low loss behaviour [1]– [3]. $Li_{0.5}Fe_{2.5}O_4$ is an inverse spinel ferrite in which Li^+ ions occupy the octahedral (B)sites and Fe^{3+} occupy the tetrahedral(A)sites of the spinel lattice [5]. Lithium and substituted lithium ferrites are useful for microwave devices such as isolators, circulars, gyrators, phase shifters, cathode materials and memory cores owing to their high Curie temperature, high resistivity, low eddy current losses, high saturation magnetization and hysteresis loop properties, which offer better performance advantage over other spinel structures [6]– [9].

Synthesis route plays a vital role on the properties of ferrites. There are many ways to synthesize ferrites like microwave hydrothermal high temp ceramic technique, flash combustion, co-precipitation, sol-gel & citrate gel methods [10]. Among all these synthesis techniques, citrate gel auto combustion method has attracted more and much attention, since this process involves a low temperature processing, homogeneity distribution of reactants and the less time, the ability to produce Nano-size particles. Several investigations on the properties of the Li–Cd [11], Li–Mg [13] and Li–Zn [12] have been reported earlier while Li-Cr has not been investigated till now.

II. EXPERIMENTAL DETAILS

2.1 Material

Lithium nitrate- $Li(NO_3)$ sigma aldrich 99% pure AR grade

Ferric Nitrate- $(Fe(NO_3)_2 9H_2O)$(98% pure GR grade),

Chromium Nitrate - $(Cr(NO_3)_2 9H_2O)$(Otto Chemie Pvt. Limited, 98%pure GR grade),

Citric acid - $(C_6H_8O_7.H_2O)$ (SDFCL-Sd fineChem. Limited, 99% pure AR grade),

Ammonia - (NH_3)(SDFCL-sd fine Chem. Limited, 99% pure AR grade) as starting materials for the synthesis.

2.2 Synthesis of Chromium Doped lithium ferrites

The synthesis of lithium ferrites nanoparticles with chromium doped compositional formula solution were prepared by mixing the stoichiometric amount of metal salts into deionized water, the required molar ratio of metal nitrates and citric acid taken and prepared by citrate gel auto-combustion method. This method has inherent advantages like low temperature (200^OC), excellent stoichiometric control, homogeneous distribution of reactants and production of fine particles with narrow size distribution. In this citrate gel auto-combustion method, metal nitrates act as oxidizing agents and organic fuels as reducing agents(19,20)the various powder properties can be systematically tuned by altering the oxidant to fuel ratios.

The stoichiometric amounts of all the nitrates were weighed and dissolved individually in a minimum amount of deionized water. All the individual solutions were added and mixed with continuous stirring for one hour on a magnetic stirrer.

The structural characterization of the synthesized samples was carried out by Philips X-ray diffractometer (Model3710) using Cu Kα radiation of wavelength 1.5405 ˚A at room temperature by continuous scanning in the range of

Bragg's angles 10 to 80 degrees in steps of 0.04 ^{0}/sec to investigate the phase and crystalline size.

The average crystalline size of the ferrites was determined from the measured using high intensity [3 1 1] peak width of their diffraction pattern using Debye Scherer's formula [14].

$D = 0.91\lambda / \beta \cos\theta$---------- (1)

Whereλ is the wavelength of the X-rays.

And β is the full width half maximum (FWHM) in radians

The lattice constant was calculated using the following relation:

$2d \sin\theta = n\lambda$---------- (2)

where $d = a/\sqrt{(h^2 + k^2 + l^2)}$

The X-ray density (dx) has been calculated according to the relation $dx = \frac{8M}{Na^3}$ [gm/cm^3] ------ (3)

where M = molecular weight of the sample. a is the lattice parameter and N is the Avogadro number. The volume of the unit cell $V = a^3$

III. RESULTS AND DISCUSSION

3.1 phase identification

The X-ray diffraction pattern of the prepared Cr substituted Lithium nano ferrites were shown in fig(1). The X-ray diffraction pattern of the prepared samples were confirmed the well-defined homogeneous single phase cubic spinel structure belonging to the space group Fd3m.The average Crystallite size of the prepared nano samples measured from the X-ray analysis line width of most intense peak (311)was in the range 27-17nm by using Debye-Scherrer's formula. The XRD analysis of the prepared Li-Cr nano crystalline samples provides the estimation of the crystallographic lattice constant (a), crystallite size (D), X-ray density (dx) and experimental density (de) etc as given in **Table 1**. It can be seen from the fig. 3 that curie temperature decreases with increase in chromium content. This confirms that the addition of chromium in lithium ferrite results in the loss of densification. A similar variation was also observed by Latta and Ravinder [15] in the case of Mn–Zn ferrites and by West and Blankenship [16] in Li–Zn ferrites.

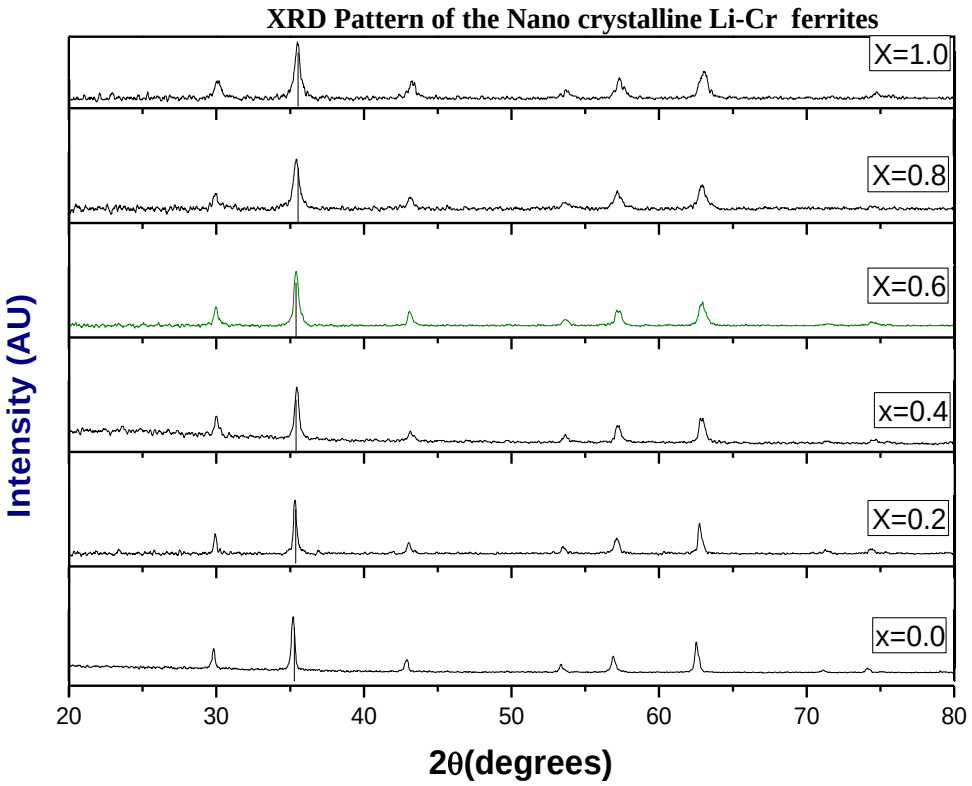

Fig. 1 XRD patterns of nanocrystalline Li-Cr ferrites

Cr-composition	Mol.Wt (gm/mole)	Crystallite size(nm)±0.2nm	Lattice parameter (A^0)	X-ray density (d_x) ±0.02	Hoping length for A-site(d_A) in A^o	Hoping length for B-site(d_B) in A^o	Porosity (%)
X=0	207.091	27	8.433	4.760	3.6080	2.9458	7.94
X=0.2	206.321	21	8.414	4.600	3.6433	2.9744	7.41
X=0.4	205.551	26	8.401	4.611	3.6328	2.9661	7.37
X=0.6	204.781	21	8.400	4.587	3.6375	2.9697	6.45
X=0.8	204.001	21	8.397	4.575	3.6361	2.9685	6.81
X=1.0	203.241	17	8.381	4.565	3.6289	2.9626	6.30

Table I. The experimental density of the prepared sample of Li-Cr Nano ferrites

3.2 DC resistivity studies

DC electrical resistivity is a useful characterization technique to understand conductivity mechanism. The DC resistivity of the samples is estimated by two probe method. A constant voltage was applied across the series combination of sample holder containing sample and a standard resistance whose value was always less than the sample resistance.

The conduction mechanism in ferrites was due to the hopping of charge carriers (electrons), between the ions of same element, present at more than one valence state, distributed randomly over equivalent crystallographic sites in lattice.

The probability of hopping hinge on the separation between the involving ions and activation energy **[**17**]**.The electrostatic interaction between the conduction electron and nearby ions may result in the polarization of the surrounding region so the electron present at the centre of the polarization well. This electron is delivered to the neighbouring site by thermal activation. This mechanism in conduction is called hopping mechanism **[**18**].**

By knowing the value of current and voltage across the sample, resistivity of the sample could be calculated by using the relation

$$\rho = RA/l \ \ \Omega\cdot cm$$

where R: Resistance of the sample, A: Surface area of the sample = πr^2

r: Radius of the sample;

For lithium ferrite, the conduction mechanism taking place between the Fe^{+2} and Fe^{+3} ions present in the equivalent crystallographic sites in the structure of the ferrite.

$$Fe^{+2} \leftrightarrow Fe^{+3} + e^-$$

In ferrites the electrons transfer between the adjacent B sites in the spinel structure. Local displacement of electrons in the direction of applied electric field can be obtained that occur due to the displacement in determining the polarization effect in ferrite **[**19**]**.

In this article we discussed the electrical conductivity of the prepared samples in the temperature range 200-600^{o}C, which reveal that the electrical conductivity of the prepared samples increases with increasing temperature, which indicated the semiconducting nature of the prepared samples. The dc electrical conductivity of the of materialshas a general form

$$\sigma = \sigma_o \exp(-E_a/kT)$$

where E_a is the thermal activation energy,

σ_o is the preexponential factor depending on nature of the material and K is the Boltzmann constant.

The temperature dependence of the electrical conductivity of the prepared samples were studied by plot a graph between the Log (σ T) vs 1000/T which shown in **Fig. 2**, which yields a straight line whose slope can be used to calculate thermal activation energies of the ferrite samples. All the plots (except pure lithium ferrites) of electrical conductivity (log σT) versus 1000/T yield a change in slope at a particular temperature. This change in slope occurs while crossing the Curie temperature (the temperature at which the ferromagnetic material changed to paramagnetic). The discontinuity at the Curie temperature was attributed to the magnetic transition from well-ordered ferromagnetic state to disordered paramagnetic state which involves different activation energies. The values of the electrical resistivity and thermal activation energies of the prepared samples in ferromagnetic region and paramagnetic region are given in **Table II**.

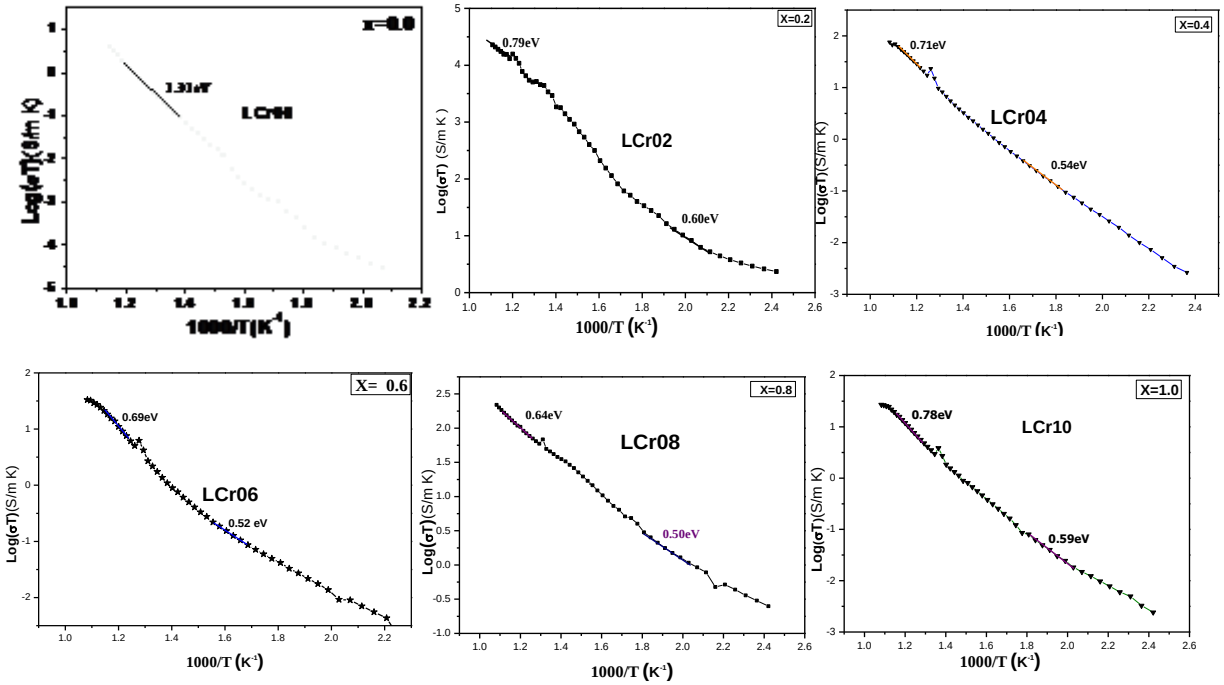

Fig. 2. Arrhenius plots for electrical conductivities of nano crystalline $Li_{0.5}Fe_{2.5-x}Cr_xO_4$ ferrites

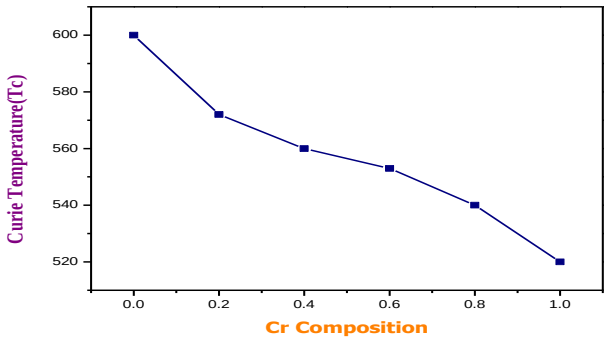

Fig. 3.Variation of Curie temperature with Cr composition.

Composition	Curie Temperature (^{o}C)	Activation Energy (eV)	
		Ferrimagnetic Region	Paramagnetic Region
$Li_{0.5}Fe_{2.5}O_4$	>600	1.34	-
$Li_{0.4}Cr_{0.2}Fe_{2.4}O_4$	572	0.875	0.945
$Li_{0.3}Cr_{0.4}Fe_{2.3}O_4$	560	0.703	0.798
$Li_{0.2}Cr_{0.6}Fe_{2.2}O_4$	553	0.526	0.659
$Li_{0.1}Cr_{0.8}Fe_{2.1}O_4$	540	0.480	0.621
$Cr_2Fe_2O_4$	520	0.575	0.712

Table. II Electrical Resistivity and Activation Energies of the $Li_{0.5}Fe_{2.5-x}Cr_xO_4$System.

3.3. Magnetic properties

Fig. 4 shows magnetic hysteresis loops for the $Li_{0.5}Fe_{2.5-x}Cr_xO_4$ (x=0.0, 0.2,0.4,0.6,0.8 and1.0) samples. Saturation magnetization (Ms), coercivity (H_C) and remanence (Mr) are listed in Table 3. While Ms and Mr decrease with increase in Cr content, H_C is found to increases. Such behaviour is attributed to the weakening of intersite exchange interaction. The coercive force (H_C) is an independent parameter that can be altered by heat treatment or deformation and hence is independent on saturation magnetization. The remnant magnetization is also an independent parameter, the values of which are seen to vary in the range23.472 to 0.118emu/g. Similar type of variation has been reported by Hankare etal. [20] in case of Li–Mn ferrites and Fu and Hsu [21] in the case of Li–Al ferrites.

composition	Coercively(Hc) (KOe)	Saturation magnetisation(Ms) (emg/g)	Remanence magnetisation(Mr) (emg/g)
0.0	105.4980	33.3470	23.472
0.2	089.6565	68.9236	11.5461
0.4	112.1303	48.1988	12.9477
0.6	114.2281	80.2320	0.4451
0.8	127.4558	62.3358	0.6527
1.0	122.9753	83.1600	0.1180

Table. III Data for coercivity (H_C), saturation magnetization(Ms), remanence magnetization(Mr) of $Li_{0.5}Fe_{2.5-x}Cr_xO_4$ system

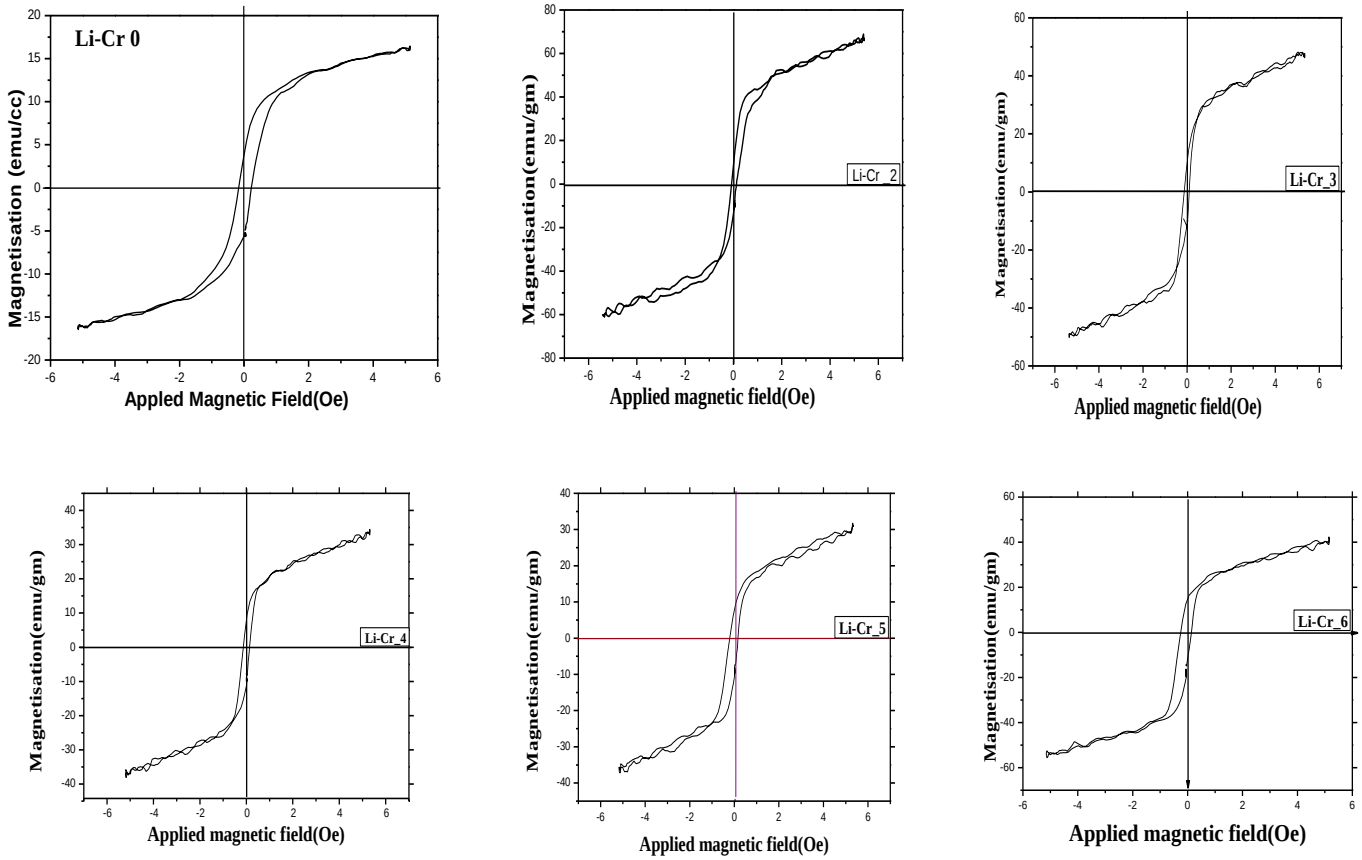

Fig. 4.Hysteresis loops for the $Li_{0.5}Fe_{2.5-x}Cr_xO_4$ samples.

IV. CONCLUSION

The Cr-substituted nano crystalline lithium ferrite samples were synthesized by citrate–gel auto combustion method.X-ray diffraction studies confirm the cubic spinel structure formation. The lattice constant and crystallite size decrease with increase in Cr content. The conduction mechanism in ferrites was due to the hopping of charge carriers. It is observed that the discontinuity in the log(σT) versus 1000/T graph shows Curiepoint of the prepared ferrite samples. Curie temperature ofthe prepared Li–Cr ferrites decreases with the increase of the Cr concentration. The saturation magnetization (Ms) and remanence (Mr) show the decreasing trend while the coercivity (H_C) shows increasing trend with increase in Cr content.

ACKNOWLEDGEMENT

The authors are very grateful to Prof. J. Siva Kumar, Head, Department of Physics, Prof. G. Prasad, Board of Studies, Department of Physics University College of Science, Osmania University, Hyderabad. Poornima B. Shetty wants to thank the management of CVR College of Engineering for their encouragement.

REFERENCES

[1] M. Abe, J. Kuroda, M. Matsumoto, J. Appl. Phys. 91(10), 7373 (2002)
[2] S.-H. Kang, H.-I. Yoo, J. Solid State Chem. 145, 276 (1999)
[3] E. Schloeman, J. Magn. Magn. Mater. 209, 15 (2000)
[4] S. Verma, P.A. Joy, J. Appl. Phys. 98 (2005) 124312.
[5] H.M. Widatallah, C. Johnson, F. Berry, M. Pekala, Solid State Commun. 120 (2001) 171.
[6] G.M. Argentina, P.D. Baba, IEEE Trans. Micro. Theory Technol. 22 (1974) 652.
[7] J.S. Baijal, S. Phanjoubam, D. Kothari, C. Prakash, P. Kishan, Solid State Commun. 83 (1992) 679.
[8] Y.P. Fu, C.S. Hsu, Solid State Commun. 134 (2005) 201.
[9] D. Ravinder, L. Balachander, Y.C. Venudhar, Mater. Lett. 49 (2001) 267.
[10] E.E.Sileo,R Roteldo S.E Jacobo J.Phy.B,320(2002),257-260
[11] S. S. Bellad, R. B. Pujar, and B. K. Chougule, *Materials Chemistry and Physics*, vol. 52, no. 2, pp. 166–169, 1998.
[12] D. Ravinder,*Journal of Materials Science Letters*, vol. 11, no. 22, pp.1498–1500, 1992.
[13] Y. Purushotham, M. B. Reddy, P. Kishan, D. R. Sagar, and P. Raghasudha, M., Ravinder, D., Veerasomaiah. P. Adv. Mat. Lett. 4, 910–916 (2013)
[14] K. Latta, D. Ravinder, Phys. Status Solidi A 139 (1993) K109.
[15] R.G. West, A.C. Blankenship, J. Am. Ceram. Soc. 50 (1967) 343.
[16] Sheenu Jauhar, Ankitha Goyal, N.Lakshmi, Kailash Chandra, Sonal Singhal, *Materials Chem and Phy*,**2013,** *139*, 836.**DOI:** 10.1016/j.matchemphys.2013.02.041
[17] Ferrite Material Science and Technology, Narosa publishing houseNew Delhi, **1990**
[18] R.K.Kontala,V.Verma,V.Pandev, V.P.S.Awana, P.P.Aloysis, P.C.Kothari, *Solid State Commun.***2007,** *143*, 527.**DOI:** 10.1016/j.ssc.2007.07.007
[19] P.P. Hankare, R.P. Patil, U.B. Sankpal, S.D. Jadhav, I.S. Mulla, K.M. Jadhav, B.K. Chougule, J. Magn. Magn. Mater. 321 (2009) 3270.
[20] Yen-Pei Fu, Chin-Shang Hsu, Solid State Commun. 134 (2005) 201.